

SCALE-LAG DIVERSITY RECEPTION IN MOBILE WIDEBAND CHANNELS

Adam R. Margetts and Philip Schniter

Dept. ECE, The Ohio State University
2015 Neil Ave, Columbus, OH 43210
{margetts.1, schniter.1}@osu.edu

Ananthram Swami

Army Research Laboratory
2800 Powder Mill Road, Adelphi, MD 20783
aswami@arl.army.mil

ABSTRACT

We consider the effect of mobility on a wideband direct sequence spread spectrum (DSSS) communication system, and study a *scale-lag* Rake receiver capable of leveraging the diversity that results from mobility. A wideband signal has a large bandwidth-to-center frequency ratio, such that the typical narrowband Doppler spread assumptions do not apply to mobile channels. Instead, we assume a more general *temporal scaling* phenomenon, i.e., a dilation of the transmitted signal's time support. Such analysis applies, for example, to ultra-wideband (UWB) radio frequency channels and underwater wideband acoustic channels.

1. INTRODUCTION

Wideband systems are defined by a ratio of single-sided bandwidth to center frequency in excess of 0.25 [1]. We are interested in studying the effect of mobility (i.e., temporal variation in the physical geometries between transmitter, receiver, and scatterers) on wideband communications systems and in designing receivers capable of leveraging the potential diversity gains that result from multipath propagation in mobile environments.

First, it is important to note that the combined effects of multipath and mobility on wideband systems are quite different than those on their narrowband counterparts. For example, in narrowband systems with a dense ring of scatterers surrounding the receiver, mobility imparts a spreading of the signal in the frequency-domain that is commonly referred to as Doppler spreading [2]. Considering a wideband system employing orthogonal frequency division multiplexing (OFDM) with narrow subcarrier bandwidths in the same physical environment, mobility implies that each subcarrier signal will experience Doppler spreading, but the amount of spreading will vary from one subcarrier to the next [3]. In wideband communication systems employing direct sequence spread spectrum (DSSS)—the focus of this manuscript—the effects of mobility in the multipath mobile environment are not well described by frequency-domain spreading, but rather by *scale spreading*.¹ By scale spreading, we mean that several copies of the transmitted signal combine at the receiver, each with a different dilation of the time support of the original signal. In addition, each copy may be temporally delayed by a different amount.

When the different propagation paths are characterized by independent dilations and delays, the fading inherent to multipath

propagation can be mitigated by using diversity reception. For wideband DSSS signaling, we study a *scale-lag Rake receiver* that exploits this diversity.² The analysis can be applied to underwater acoustic systems [5] as well as to radio frequency ultra-wideband (UWB) systems [6].

2. SYSTEM MODEL

2.1. Transmit Signal

The wideband DSSS waveform is

$$x(t) = \frac{1}{\sqrt{N_p}} \sum_{i=0}^{N_p-1} c_i p(t - iT_o), \quad (1)$$

where $\{c_i\}$ is the length- N_p PN chip sequence, $p(t)$ is the unit-energy chip waveform, and T_o is the chip duration. The symbol duration is $T_s = N_p T_o$ seconds and the system bandwidth is defined to be $W = 1/T_o$. A PN sequence chosen from a ternary alphabet $\{-1, 0, 1\}$ may be used to model time-hopping [6] or episodic signaling [7] without affecting the analysis. In this paper, we consider only baseband signaling; thus, all signals and parameters are real valued. We linearly modulate the DSSS waveform $x(t)$ with a sequence of N_b symbols $\{b_j\}$ to obtain the transmitted signal.

2.2. Wideband Channel Kernel

Analogous to the spreading function in narrowband signaling, the wideband signal input-output relationship can be modelled by the linear transformation $y(t) = \mathcal{L}\{x(t)\}$ [4] defined by:

$$y(t) = \int \int \mathcal{L}(a, \tau) \frac{1}{\sqrt{a}} x\left(\frac{t - \tau}{a}\right) da d\tau, \quad (2)$$

where $x(t)$ is the channel input and $\mathcal{L}(a, \tau)$ is the *wideband channel kernel*. Note that the wideband channel transformation is *not* shift-invariant; hence, sinusoids are *not* eigenfunctions. The wideband channel kernel $\mathcal{L}(a, \tau)$ quantifies the scale-lag spreading produced by the channel—the variable a corresponds to the dilation introduced by the channel, and the variable τ corresponds to the propagation delay.

We illustrate the wideband channel kernel with the simple two-path, lossless channel shown in Fig. 1. Suppose that the two paths have equal length: $d = c\tau_d$, where c is the speed of wave propagation and τ_d is the temporal lag from transmitter to receiver.

This work was supported in part by the Ohio Space Grant Consortium and by Army Research Laboratory.

¹Note that scale-spreading is actually a general concept that applies to both narrowband and wideband systems. For example, changing the time scale of a sinusoidal signal is equivalent to shifting the signal in frequency.

²The possibility of a scale-lag receiver was mentioned in [4], but no details were developed.

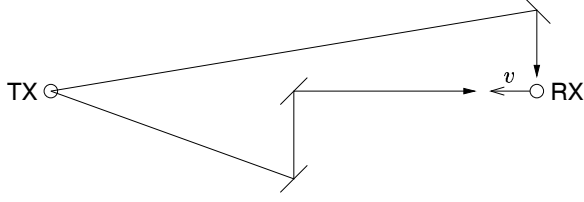


Fig. 1. Wireless channel diagram with two equal-length propagation paths from the transmitter to the receiver. The receiver is traveling with velocity v .

The signal arriving perpendicular to the direction of motion experiences no dilation ($a = 1$), while the signal arriving parallel to the direction of motion experiences a dilation of $a_o < 1$. Hence, the received signal is $y(t) = x(t - \tau_d) + \frac{1}{\sqrt{a_o}}x\left(\frac{t - \tau_d}{a_o}\right)$, where $x(t)$ is the transmitted signal. In this case, the wideband channel kernel can be written $\mathcal{L}(a, \tau) = \delta(a - 1)\delta(\tau - \tau_d) + \delta(a - a_o)\delta(\tau - \tau_d)$, where $\delta(\cdot)$ is the Dirac delta function.

To simplify the following exposition, we assume a mobile receiver, fixed reflectors, and a fixed transmitter.³ In a rich scattering environment, the wideband channel kernel $\mathcal{L}(a, \tau)$ is non-zero on a continuum of points (a, τ) . However, finite mobile velocity implies that the temporal scaling is bounded: $\{(a, \tau) : a_{min} < a < a_{max}, 0 < \tau < \tau_{max}\}$, where a_{min} and a_{max} are the minimum and maximum dilation, respectively, and τ_{max} is the delay spread. By convention, the time delay of the shortest path is zero lag.

Relativistic effects for electromagnetic wave propagation are negligible due to low mobile velocities; hence, the minimum dilation and maximum dilation can be simplified to $a_{min} = 1 - v_{max}/c$ and $a_{max} = 1 + v_{max}/c$, respectively, where v_{max} is the maximum mobile velocity [8]. An important system parameter is the wideband scale spread: $\gamma_{max} := \frac{a_{max} - a_{min}}{2} = v_{max}/c = a_{max} - 1$, which defines the maximum deviation from unit temporal dilation. Though typical values of γ_{max} may be extremely small for mobile RF channels, we establish, in the sequel, that wideband DSSS signals can be very sensitive to this parameter.

We assume the symbol duration T_s is much larger than the delay spread τ_{max} ; hence, we can ignore inter-symbol interference and without loss of generality assume one-shot transmission. Let $x(t)$ be linearly modulated by a data symbol b with energy E_b . The received signal $r(t)$ in additive white Gaussian noise $w(t)$ with two-sided power spectral density of $N_o/2$ is

$$r(t) = \mathcal{L}\{bx(t)\} + w(t), \quad (3)$$

$$= by(t) + w(t). \quad (4)$$

The optimal receiver, assuming no inter-symbol interference (ISI), is the matched filter, which requires knowledge of the wideband channel kernel $\mathcal{L}(a, \tau)$.

2.3. Scale-Lag Resolution

The scale-lag resolution properties of a wideband DSSS signal $x(t)$ are related to the total signal bandwidth W and symbol duration T_s . An often used rule-of-thumb is that the minimum resolvable lag of a linear Rake receiver is $T_o = 1/W$ [2]. A similar

³The wideband kernel can be used to model any dynamic geometry between the transmitter, scatters, and receiver, e.g., a turbulent underwater environment with rings of scatters moving at different speeds.

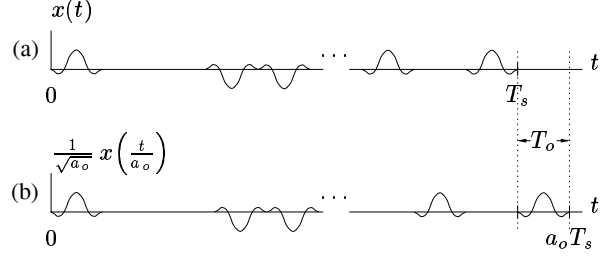


Fig. 2. (a) Transmitted wideband signal. (b) Signal dilated by a_o .

rule-of-thumb can be suggested for the *minimum resolvable dilation*, which will be defined next.

Consider the inner product of $x(t)$ with $x(t)$ dilated by a :

$$\left\langle x(t), \frac{1}{\sqrt{a}}x\left(\frac{t}{a}\right) \right\rangle. \quad (5)$$

Let $a = a_o$ result in a dilation by one chip period, (illustrated by Fig. 2) or in other words, let a_o satisfy the relation

$$a_o T_s - T_s = T_o \Leftrightarrow a_o = 1 + 1/N_p. \quad (6)$$

Proposition 1. The expected value of the inner product (5) evaluated at $a = a_o$ vanishes if and only if the pulse-shape has zero DC component.

Proof. The proof is found in Appendix A. \square

Hence, we define a_o as the *minimum resolvable dilation*. Equivalently, $\gamma_o := a_o - 1$ is the *scale resolution* of the wideband DSSS signal $x(t)$. We have $\gamma_o = T_o/T_s = 1/T_s W = 1/N_p$, i.e., the scale resolution is the inverse of the time-bandwidth product or spreading gain.

2.3.1. Discussion

The ratio $\frac{\gamma_{max}}{\gamma_o}$ is the *normalized scale spread* and can be written in terms of the velocity, speed of signal propagation, and the time-bandwidth product: $\frac{\gamma_{max}}{\gamma_o} = \frac{v_{max}}{c} T_s W$. Note the similarity to the narrowband normalized Doppler-frequency spread [2]: $f_d T_s = \frac{v_{max}}{c} T_s f_c$, where f_c is the carrier frequency.

2.4. Choice of Basis Functions

Since estimation of the continuous-valued kernel $\mathcal{L}(a, \tau)$ is difficult, we project the received signal $r(t)$ onto basis $\{x_{m,n}(t)\}$:

$$r_{m,n} = \langle x_{m,n}(t), r(t) \rangle, \quad (7)$$

$$= by_{m,n} + w_{m,n}, \quad (8)$$

where $y_{m,n} = \langle x_{m,n}(t), y(t) \rangle$ are the signal coefficients and $w_{m,n} = \langle x_{m,n}(t), w(t) \rangle$ are the noise coefficients. A coherent receiver estimates the basis coefficients $\{y_{m,n}\}$ for use in the scale-lag rake combiner.

From the scale-lag resolution properties of Sec. 2.3, and to match the scale-lag spreading of the wideband channel, it is natural to choose as basis functions the set of dilated-delayed versions of the transmitted signal:

$$x_{m,n}(t) = \frac{1}{\sqrt{a_o^n}} x\left(\frac{t - nT_o}{a_o^n}\right). \quad (9)$$

Together, the scale-lag resolution properties of the basis signals imply that $\langle x_{m,n}(t), x_{\bar{m},\bar{n}}(t) \rangle \approx \delta_{m-\bar{m},n-\bar{n}}$, where $\delta_{m,n}$ is the Kronecker delta function. Note that the projection is an implicit approximation of the wideband kernel

$$\mathcal{L}(a, \tau) \approx \sum_{m,n} \ell_{m,n} \delta(a - a_o^m) \delta(\tau - nT_o). \quad (10)$$

The coefficients $\{r_{m,n}\}$ are effectively a sampling of the scale-lag plane, as shown in Fig. 3. A Taylor's series approximation around $a_o = 1$ gives $a_o^m \approx 1 + m(a_o - 1) = 1 + m\gamma_o$; hence, a uniform spacing in the scale domain suffices for typical values of dilation (i.e., $a \approx 1$).

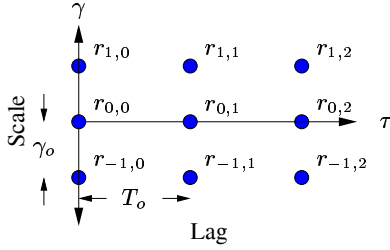


Fig. 3. Sampling the scale-lag plane.

3. SCALE-LAG DIVERSITY

To determine the diversity exploited by the coherent scale-lag Rake receiver, we compile the basis coefficients, $\{y_{m,n}\}$, $-M \leq m \leq M$ and $0 \leq n \leq N$, into a vector, compute the autocorrelation matrix by taking the expected outer-product, and examine the eigenvalues $\{\lambda_i\}$. The values M and N are chosen so that a significant portion of the energy is contained in the basis coefficients.

Assuming the wideband channel kernel is uncorrelated across scale and lag⁴, i.e., $E[\mathcal{L}(a, \tau)\mathcal{L}(a', \tau')] = \Psi(a, \tau)\delta(a - a')\delta(\tau - \tau')$, where $\Psi(a, \tau)$ is the *scattering function*, we obtain the elements of the expected outer product,

$$E[y_{m,n}y_{\bar{m},\bar{n}}] = \int_0^{\tau_{max}} \int_{1-\gamma_{max}}^{1+\gamma_{max}} \Psi(a, \tau) \chi\left(a_o^m/a, \frac{nT_o - \tau}{a}\right) \chi\left(a_o^{\bar{m}}/a, \frac{\bar{n}T_o - \tau}{a}\right) da d\tau \quad (11)$$

where $\chi(a, \tau) = \int x(t) \frac{1}{\sqrt{a}} x\left(\frac{t-\tau}{a}\right) dt$ is the *wideband ambiguity function* (similar to [10]).

The BER expression, assuming the coefficients fade according to a real-valued Gaussian distribution, is

$$P_e = \frac{1}{\pi} \int_0^{\pi/2} \prod_{i=0}^{\kappa-1} \left(\frac{2E_b\lambda_i}{N_o \sin^2 \theta} + 1 \right)^{-1/2} d\theta, \quad (12)$$

$$\leq \frac{1}{2} \prod_{i=0}^{\kappa-1} \left(\frac{2E_b\lambda_i}{N_o} + 1 \right)^{-1/2}. \quad (13)$$

where $\kappa = (2M + 1)(N + 1)$.

⁴This simplifying assumption is somewhat analogous to the uncorrelated doppler-lag spreading assumption made in narrowband systems [9].

3.1. Approximation

For the unit-energy second-derivative Gaussian pulse⁵,

$$p(t) = \frac{\sqrt{f_o} \sqrt[4]{32\pi}}{\sqrt{3}} [1 - 2(\pi f_o(t - T_o/2))^2] \exp(-(\pi f_o(t - T_o/2))^2), \quad (14)$$

it can be shown [11] that for large N_p , the autocorrelation (11) can be approximated by

$$E[y_{m,n}y_{\bar{m},\bar{n}}] \approx \int_0^{\frac{\tau_{max}}{T_o}} \int_{-\frac{\gamma_{max}}{\gamma_o}}^{\frac{\gamma_{max}}{\gamma_o}} \Psi(1 - \gamma_o\delta, \bar{\tau}T_o) \bar{\chi}(m + \delta, n - \bar{\tau}) \bar{\chi}(\bar{m} + \delta, \bar{n} - \bar{\tau}) d\delta d\bar{\tau}, \quad (15)$$

where, for $f_o = 2/T_o$, we have

$$\bar{\chi}(\delta, \bar{\tau}) = \frac{1}{12} \sum_{k=0}^4 w_k \int_0^1 x^k e^{-2\pi^2(\delta x + \bar{\tau})^2} dx, \quad (16)$$

$$\begin{aligned} w_0 &= 12 - 96\pi^2\bar{\tau}^2 + 64\pi^4\bar{\tau}^4, \\ w_1 &= 256\pi^4\bar{\tau}^3\delta - 192\pi^2\bar{\tau}\delta, \\ w_2 &= 24(16\pi^4\bar{\tau}^2\delta^2 - 4\pi^2\delta^2), \\ w_3 &= 256\pi^4\bar{\tau}\delta^3, \\ w_4 &= 64\pi^4\delta^4. \end{aligned}$$

4. SCALE-LAG RAKE RECEIVER PERFORMANCE

We use the approximation (15) to compute the eigenvalues $\{\lambda_i\}$ of a system employing a second-derivative Gaussian pulse shape. For simplicity, we assume the scattering function $\Psi(a, \tau)$ is flat across scale and lag, and fix the delay spread to be $\tau_{max} = T_o$. We choose $M = \left\lfloor \frac{\gamma_{max}}{\gamma_o} \right\rfloor + 1$ and $N = \left\lfloor \frac{\tau_{max}}{T_o} \right\rfloor + 1$ to capture a significant portion of the received energy in the basis coefficients. Fig. 4 displays the eigenvalues⁶ of the basis-coefficient autocorrelation matrix for various values of normalized scale spread. For a normalized scale spread below 0.1, the scale-lag rake exploits an essential diversity order of four, i.e., over the SNR of interest, only the first four eigenvalues contribute to a reduction in bit error rate (BER). At a scale spread of 1.0, the scale-lag rake exploits six levels of diversity.

Figure 5 compares the BER performance of the scale-lag Rake to a conventional Rake using the system parameters of the preceding paragraph. Note that a higher value of scale spread produces a greater performance gap between the scale-lag Rake and the conventional Rake, as predicted by the preceding diversity analysis. Also note the decrease in performance of the conventional Rake at a higher value of normalized scale spread since a larger proportion of the received energy is in the scale components.

A normalized scale spread of 0.001 would be found in an RF system with mobile velocity of 10 km/hr, data rate of 10 kbps, and bandwidth of 1 GHz, or in an RF system with velocity of 100 km/hr, data rate of 1 Mbps, and bandwidth of 10 GHz. A normalized scale spread of 1.0 would be found in an underwater acoustic telemetry system with mobile velocity of 15 km/hr, data rate of 100 bps, and bandwidth of 36 kHz.

⁵We wish to point out that other zero-DC component signals may be used, such as the modified duobinary pulse [2].

⁶The eigenvalues for each given scale spread have been normalized to unit energy, i.e., their sum is unity.

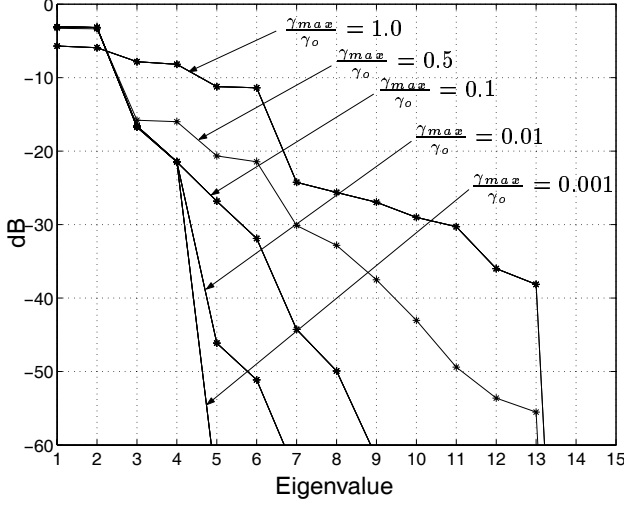


Fig. 4. Eigenvalues of basis coefficient autocorrelation matrix.

5. CONCLUSION

In this paper, we studied a *scale-lag* Rake receiver capable of leveraging the diversity that results from scale-lag spreading in mobile wideband DSSS systems. The analysis applies to channels where narrowband assumptions are invalid, such as radio-frequency UWB systems and wideband hydro-acoustic systems. Future work includes investigating the implementation details of the scale-lag Rake and estimating the basis coefficients for coherent combining.

A. PROOF OF PROPOSITION 1.

Assuming the PN sequence is i.i.d. and the pulse-shape is zero outside the interval $[0, T_o]$, we can write

$$\begin{aligned} \mathbb{E} \left[\left\langle x(t), \frac{1}{\sqrt{a}} x\left(\frac{t}{a}\right) \right\rangle \right] &= \mathbb{E} \left[\int_{-\infty}^{\infty} x(t) \frac{1}{\sqrt{a}} x\left(\frac{t}{a}\right) dt \right], \\ &= \sum_{i=0}^{N_p-1} \frac{\mathbb{E} |c_i|^2}{N_p \sqrt{a}} \int_0^{T_o} p(t)p\left(\frac{t + (1-a)iT_o}{a}\right) dt. \\ &= \sum_{i=0}^{N_p-1} \frac{\mathbb{E} |c_i|^2}{N_p \sqrt{a}} \chi_p(a, (1-a)iT_o) \end{aligned} \quad (17)$$

where $\chi_p(a, \tau) = \int p(t) \frac{1}{\sqrt{a}} p\left(\frac{t-\tau}{a}\right) dt$ is the ambiguity function of the pulse shape. Now plug the value $a = a_o = 1 + 1/N_p$ into (17) and let N_p go to infinity

$$\begin{aligned} \lim_{N_p \rightarrow \infty} \sum_{i=0}^{N_p-1} \frac{\mathbb{E} |c_i|^2}{N_p} \chi_p\left(1 + \frac{1}{N_p}, \frac{iT_o}{N_p}\right) \\ \approx \frac{\mathbb{E} |c_i|^2}{T_o} \int_0^{T_o} R_{p,p}(x) dx, \\ = \frac{\mathbb{E} |c_i|^2}{2T_o} S_p(0), \end{aligned} \quad (18)$$

where $R_{p,p}(x)$ is the deterministic autocorrelation function of the pulse-shape, and $S_p(f)$ is the power spectral density. From (18),

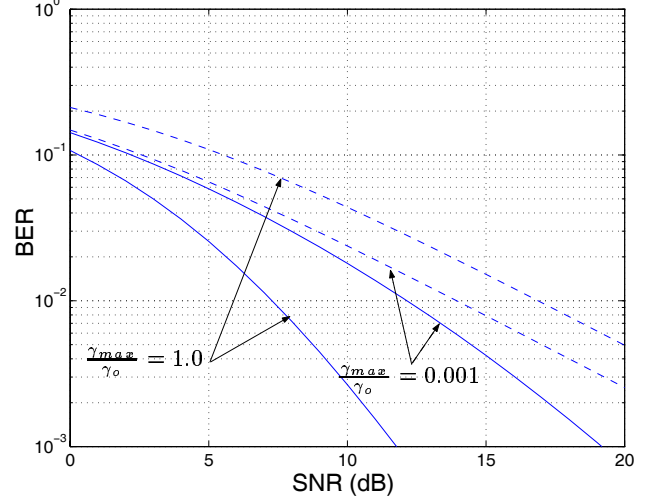


Fig. 5. (Solid) BER performance of scale-lag Rake receiver. (Dashed) BER performance of conventional Rake. The normalized delay spread is $\tau_{max}/T_o = 1$. Only the basis coefficients corresponding to zero scale ($m = 0$) are used to compute the performance of the conventional rake receiver.

we conclude that the expected value of the inner-product (5) vanishes at the minimum resolvable dilation a_o if and only if the *pulse-shape has no DC component*.

B. REFERENCES

- [1] J. Taylor, "Ultrawideband radar," *IEEE MTT-S International Microwave Symposium Digest*, vol. 1, pp. 367–370, Jun. 1991.
- [2] J. Proakis, *Digital Communications*. New York, NY: McGraw-Hill, 3rd ed., 1995.
- [3] A.-B. Salberg and A. Swami, "Doppler and frequency-offset synchronization in wideband OFDM," *IEEE Trans. on Wireless Communications*, accepted for publication.
- [4] R. Balan, H. V. Poor, S. Rickard, and S. Verdú, "Time-frequency and time-scale canonical representations of doubly spread channels," *Proc. European Signal Processing Conf.*, Sep. 2004.
- [5] J. Davies, S. Pointer, and S. Dunn, "Wideband acoustic communications dispelling narrowband myths," *OCEANS 2000 MTS/IEEE Conference and Exhibition*, vol. 1, pp. 377–384, Sep. 2000.
- [6] M. Win and R. Scholtz, "Ultra-wide bandwidth time-hopping spread-spectrum impulse radio for wireless multiple-access communications," *IEEE Trans. on Communications*, vol. 48, pp. 679–689, Apr. 2000.
- [7] B. M. Sadler and A. Swami, "On the performance of episodic UWB and direct-sequence communication systems," *IEEE Trans. on Wireless Communications*, 2004, accepted for publication.
- [8] S. Rickard, *Time-frequency and time-scale representations of doubly spread channels*. PhD thesis, Princeton University, November 2003.
- [9] A. M. Sayeed and B. Aazhang, "Joint multipath-doppler diversity in mobile wireless communications," *IEEE Trans. on Communications*, vol. 47, pp. 123–132, Jan. 1999.
- [10] D. Swick, "Wideband ambiguity function of pseudo-random sequences: An open problem," *IEEE Trans. on Information Theory (correspondence)*, July 1968.
- [11] A. R. Margetts and P. Schniter, "Joint scale-lag diversity in mobile wideband communication systems," *Journal Manuscript in Preparation*.